

RAPIDLY TIME VARIABLE PHENOMENA: JETS, EXPLOSIVE EVENTS, AND FLARES

K. Shibata

National Astronomical Observatory of Japan, Mitaka, Tokyo 181, Japan

ABSTRACT

Recent observations and related theoretical works on rapidly time variable phenomena such as jets, explosive events, flares, etc., are reviewed with emphasis on the role of magnetic reconnection. The phenomena discussed in this paper include X-ray jets, H α surges, EUV jets/explosive events, transient brightenings (microflares), X-ray plasmoid ejections, H α filament eruptions, and flares. Many of observational material are from Yohkoh soft X-ray observations, including also ground based observations coordinated with Yohkoh. A unified model based on the magnetic reconnection hypothesis is presented to understand these (apparently different) phenomena.

Key words: jets; flares; reconnection; MHD.

1. INTRODUCTION

The soft X-ray telescope (SXT) (Tsuneta et al. 1991, Acton et al. 1992) aboard Yohkoh (Ogawara et al. 1991) has revealed that the solar corona is much more dynamic than had been thought, and discovered various dynamic phenomena such as *transient brightenings* (soft X-ray (SXR) microflares) (Shimizu et al. 1992, 1994, Shimizu 1995, 1996), *X-ray jets* (Shibata et al. 1992b, 1994a,b, 1996, Strong et al. 1992, Shimojo et al. 1996), *X-ray plasmoid ejections* (Shibata et al. 1995, Nitta 1996, Ohya and Shibata 1997a,b, Tsuneta 1997), and so on. These dynamic phenomena are closely related to magnetic reconnection, and could be important not only in understanding coronal heating and acceleration of high speed solar wind (e.g., Brueckner and Bartoe 1983), but also in clarifying fundamental physics of magnetic reconnection (e.g., Ono et al. 1996, Biskamp 1997, Tajima and Shibata 1997).

In this paper, we shall review these new Yohkoh observations and related theoretical studies with emphasis on the role of magnetic reconnection. In particular, it is stressed that unified view has emerged on apparently different phenomena, ranging from microflares to large scale flares. We argue that even EUV explosive events/jets (e.g., Dere et al. 1991) and spicules (e.g., Suematsu et al. 1995, Sterling et al. 1993) might be unified in the same line of thought. Future observations using SOHO instru-

ments are also suggested, e.g., to detect Doppler shift velocity of X-ray jets, X-ray plasmoid ejections, etc.

2. MICROFLARES AND JETS

2.1. TRANSIENT BRIGHTENINGS (MICROFLARES)

Shimizu et al. (1992, 1994) analyzed active region transient brightenings (ARTBs) in detail, and found that these correspond to soft X-ray counter part of hard X-ray microflares (Lin et al. 1984, Dennis 1985). The total thermal energy content of ARTBs is $10^{25} - 10^{29}$ erg, their lifetime ranges from 1 to 10 min, their length is $(0.5 - 4) \times 10^4$ km, and the temperature is about 6 - 8 MK. According to recent analysis by Shimizu (1996) on the comparison of Yohkoh SXT images of ARTBs with simultaneous visible light observations at LaPalma, some ARTBs occur in association with emergence of tiny magnetic bipoles, suggesting the reconnection between emerging flux and pre-existing field.

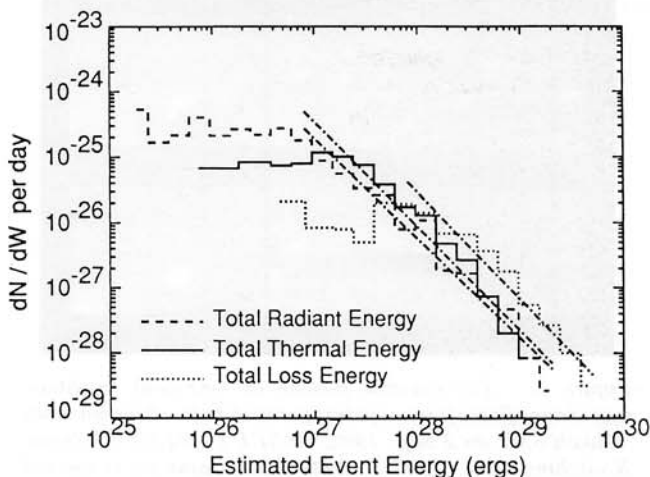


Figure 1. Frequency distribution of transient brightenings (microflares) as a function of the total energy estimated with three different methods (taken from Shimizu 1995). Each distribution can be represented by a single power law with the index 1.5 - 1.6 (dash-dotted lines).

The occurrence frequency of these ARTBs (SXR mi-

croflares) decreases with increasing their total energy and shows power-law distribution;

$$dN/dE \propto E^{-\alpha},$$

where dN is the number of ARTBs per day in the energy range between $E + dE$ and E , and $\alpha \simeq 1.5 - 1.6$ (Shimizu 1995; see Fig. 1). This is nearly the same as that of hard X-ray (HXR) microflares and larger flares. Since the index α is less than 2, the SXR microflares alone cannot explain coronal heating.¹ The universal power-law distribution seems to suggest the universal physical origin of both microflares and large scale flares (Watanabe 1994).

From simultaneous observations by VLA and Yohkoh, Gopalswamy et al. (1994) found microwave counterparts of ARTBs. Kundu et al. (1994) observed type III bursts in association with an XBP flare, which means that XBP flares are similar to normal flares and can accelerate nonthermal electrons.

Recently, Koutchmy et al. (1997a,b) have found even less energetic transient brightenings in polar regions, which they call *coronal flashes*. The absolute SXR intensity of flashes is about 10 DN/s at maximum, which is two orders of magnitude smaller than those of ARTBs, and fluctuates on a time scale of a few - 5 min. The total (released) energy is probably comparable to 10^{24} erg, i.e., that of nanoflares. The polar coronal holes are found to be very active and full of these nanoflares, and even tiny X-ray jets often occur from these nanoflares (see Fig. 2).

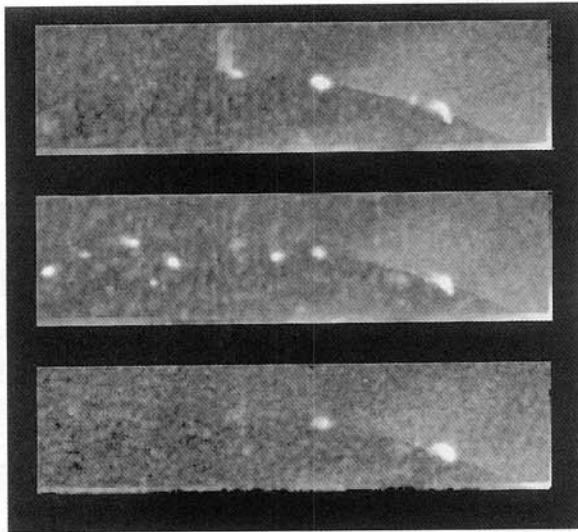


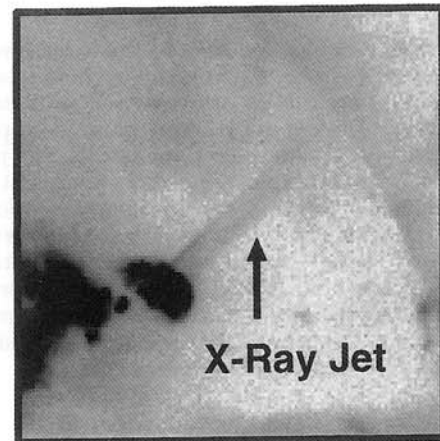
Figure 2. The coronal flashes or transient brightenings (nanoflares) in a polar coronal hole observed with Yohkoh SXT on 2 Sep. 1992, 00:31 UT - 04:07 UT (from Koutchmy et al. 1997b). Note that a faint jet is ejected vertically from one of brightenings. These images are summation of many images taken during each satellite orbit (daytime < 60 min).

2.2. X-RAY JETS

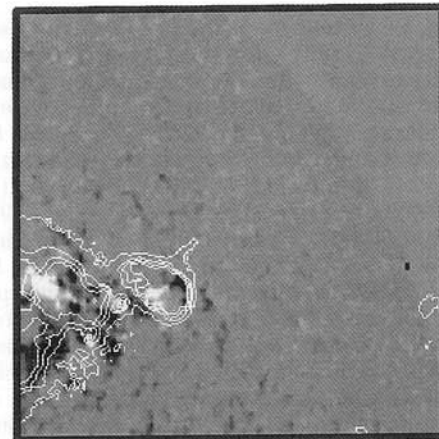
X-ray jets are defined as transitory X-ray enhancements with apparent collimated motion (Shibata et

¹Porter et al. (1990), however, claimed that EUV microflares show the power law index larger than 2.

al. 1992b, 1994a,b, 1996, Strong et al. 1992, Shimajo et al. 1996). Almost all jets are associated with microflares or subflares, and the length ranges from 1000 to 4×10^5 km. No one knows their true (Doppler shift) velocity; their apparent velocity is 10 - 1000 km/s. To measure Doppler shift velocity of X-ray jets would be one of the most important subjects for SOHO SUMER or CDS. The temperature of X-ray jets is about 4 - 6 MK, which is comparable to those of the footpoint microflares. The electron density ranges from 3×10^8 to 5×10^9 cm⁻³ and the kinetic energy was estimated to be $10^{25} - 10^{29}$ erg. Figure 3 shows a typical example of X-ray jets with a length $\sim 2 \times 10^5$ km and a velocity of more than 100 km/s.



Yohkoh SXT Image
12-Nov-91 11:30UT



Kitt-Peak Magnetogram
12-Nov-91 16:07UT

Figure 3. Top: An X-ray jet observed with Yohkoh SXT on 12 Nov. 1991 (Shibata et al. 1992b). Bottom: NSO/Kitt Peak magnetogram for the same region with overlay of contours of soft X-ray intensity distribution. Note mixed polarities at the footpoint of the jet.

Figure 4 shows histograms of length and velocity of jets. Note that the number of jets decrease with increasing length and velocity. Interestingly, the shape of these histogram is quite similar to those of EUV jets (Cook and Brueckner 1991).

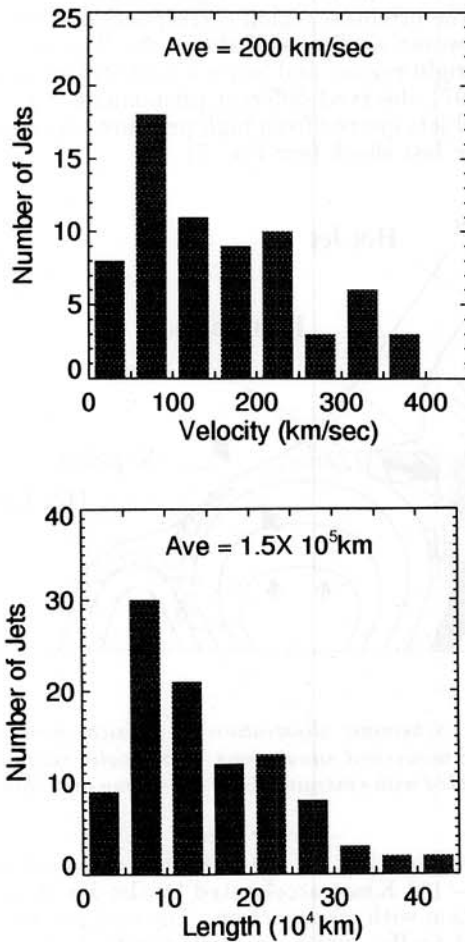


Figure 4. Histograms of velocity and length of X-ray jets (from Shimojo et al. 1996).

There are a number of evidence of magnetic reconnection in X-ray jets.

(1) Morphology: Many jets show constant or converging shape (Shimojo et al. 1996), implying the magnetic field configuration with a neutral point near the footpoint of a jet as shown in Figure 5. In some jets, a gap is seen between footpoints of jets and brightest part of the footpoint flares. This is also explained by the reconnection model (Shimojo et al. 1996), since the reconnection creates two hot reconnected field lines (a loop and a jet) with a gap between them. Shibata et al. (1994a) noted that there are two types of interaction between emerging flux and overlying coronal field; one is the *anemone-jet* type, in which emerging flux appears in a coronal hole and a jet is ejected vertically, and the other is the *two-sided-loop* type, which occurs when the emerging flux appears in a quiet (closed loop) region, producing two-sided loops (or jets). The morphology of these types suggests the reconnection between emerging flux and overlying coronal field and resulting formation of jets (or loop brightenings).

(2) Magnetic field: Shimojo, Harvey, and Shibata (1997) have revealed that the magnetic field properties of the footpoint of jets are mainly mixed polarities or satellite spots. This gives direct evidence of the presence of neutral points (or current sheets)

near the footpoint of jets.

(3) $H\alpha$ surges: Often $H\alpha$ surges are associated with X-ray jets (e.g., Shibata et al. 1992b, Canfield et al. 1996), though there are also negative cases (e.g., Schmieder et al. 1995). From observations of $H\alpha$ surges associated with X-ray jets, Canfield et al. (1996) found several new evidence of reconnection.

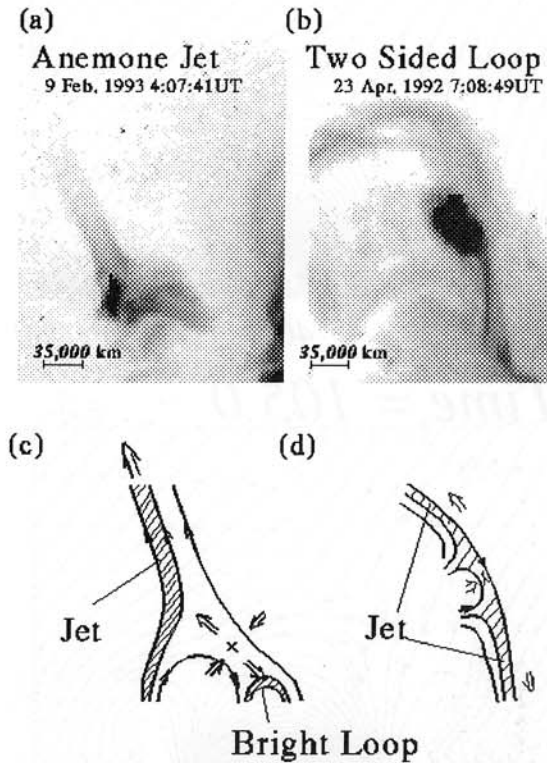


Figure 5. Two types of interaction between emerging flux and overlying coronal field (from Yokoyama and Shibata 1996).

(4) Type III bursts: Kundu et al. (1995) found that some X-ray jets are associated with type III bursts (see also Auras et al. 1995, Raulin et al. 1996). This indicates that high energy electrons are accelerated in these small scale microflare/jet events, suggesting that the same physical process as that of larger flares (i.e., magnetic reconnection) might be occurring in these events.

2.3. MAGNETIC RECONNECTION MODEL: EMERGING FLUX MODEL

Yokoyama and Shibata (1995, 1996) developed magnetic reconnection model of X-ray jets using 2.5D MHD numerical simulations (Fig. 6). In their model, magnetic reconnection occurs in the current sheet between emerging flux and overlying coronal field as in the classical emerging flux model (Heyvaerts et al. 1974, Forbes and Priest 1984, Shibata et al. 1992a). The basic driving force is magnetic buoyancy, though the reconnection rate is not uniquely determined by the external condition (i.e., rise velocity of emerging flux) but is affected by the local plasma condition such as the resistivity and dynamics (Ugai 1986, 1994, Scholer 1989, Yokoyama and Shibata 1994). Yokoyama and Shibata (1995, 1996) found several

interesting features in their simulation results based on emerging flux model.

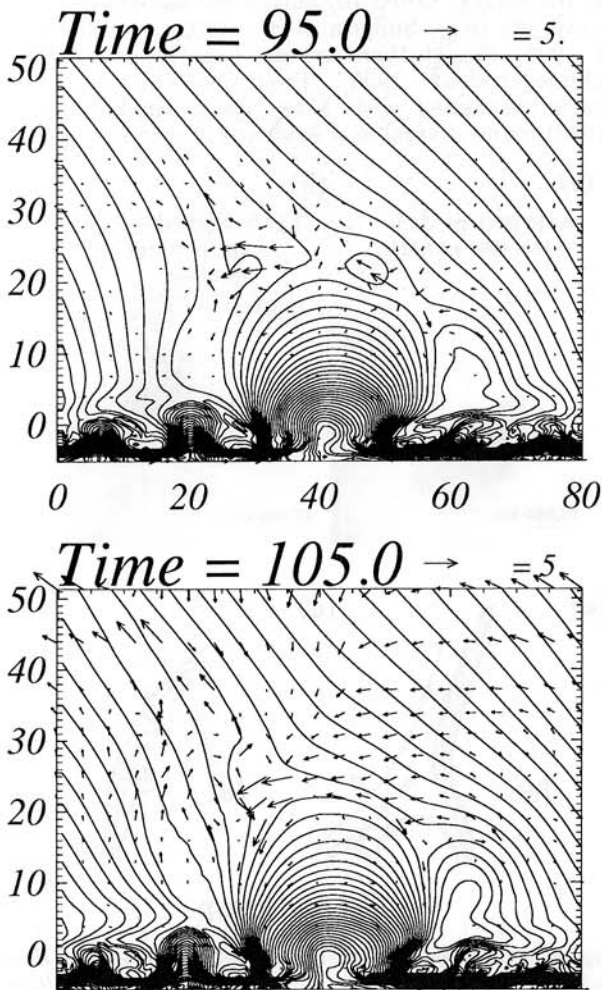


Figure 6. Emerging flux reconnection model of Yokoyama and Shibata (1995, 1996). Note that plasmoids (magnetic islands) are repeatedly created in the current sheet.

(1) The reconnection starts with the formation of magnetic islands (i.e., plasmoids). (In three dimension, they are seen as helically twisted flux rope.) These islands coalesce with each other and finally are ejected out of the current sheet. After the ejection of the biggest island, the largest energy release occur.

(2) The reconnection jets from the X-point soon collides with the ambient field to form fast shocks. The global jets are emanating from the high pressure region just behind the fast shock, and propagate along the reconnected field line. This suggests that *observed X-ray jets are not the reconnection jet itself, but hot jets accelerated by the enhanced gas pressure behind the fast shock.*

(3) The emission measure is the smallest at the X-point, since the volume of the X-point is very small (Yokoyama and Shibata 1996). Thus the X-point is not bright and hence is not easy to be detected. This may be the reason why we observe a gap between a jet and the brightest part of a footpoint flare. In relation to this, Innes et al. (1997) recently reported interesting observations of bi-directional plasma jets using SOHO/SUMER. They interpreted that these jets corresponded to reconnection jets because the in-

tensity between two jets was largest and hence (they thought) the brightest region corresponded to the X-point. However, as discussed above, the X-point cannot be a bright region, and hence it is likely that Innes et al. (1997) observed different phenomena, e.g., bi-directional jets ejected from high pressure region just behind the fast shock (see Fig. 7).

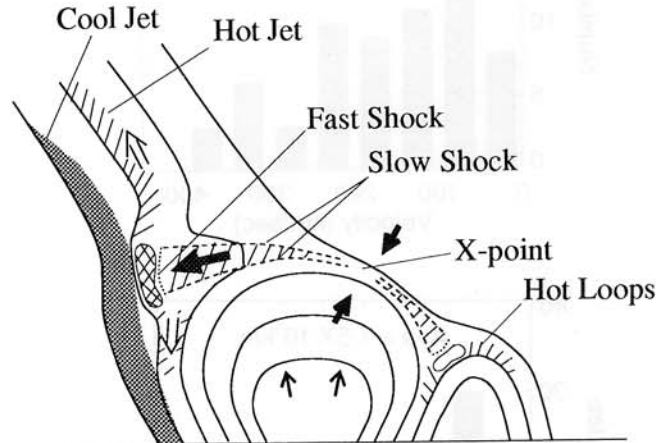


Figure 7. Schematic illustration of physical processes found from numerical simulations of magnetic reconnection associated with emerging flux (Yokoyama and Shibata 1996).

(4) Not only hot jets ($T > 10^6$ K) but also cool jets ($T \sim 10^4 - 10^5$ K) are accelerated by the $\mathbf{J} \times \mathbf{B}$ force in association with reconnection. The cool jets might correspond to $H\alpha$ surges associated with X-ray jets (Shibata et al. 1992b, Canfield et al. 1996, Okubo et al. 1997). These cool jets start to be accelerated just before hot jets are formed, and are ejected originally as plasmoids (or helically twisted flux rope in three dimension) and form an elongated structure after the plasmoids collides with ambient fields. The initial phase of the ejection of both cool and hot jets are seen as *whip-like motion*. In main phase, the cool jets are situated just side of the hot jets with nearly the same orientation. These features are indeed observed in several $H\alpha$ surges associated with X-ray jets (Canfield et al. 1996).

(5) Okubo et al. (1996) extended Yokoyama and Shibata (1996)'s simulations to the case in which twisted or sheared magnetic flux emerges to reconnect with overlying field. They found that as a result of reconnection between twisted (sheared) field and untwisted field, shear Alfvén waves are generated and propagate along reconnected field lines. Since these Alfvén waves have large amplitude, they excite large transversal motion (or spinning motion) of jets and exert nonlinear magnetic pressure force to cool/hot jets to cause further acceleration of them, as originally suggested by Shibata and Uchida (1986) (see Fig. 8). Canfield et al. (1996) found that all $H\alpha$ surges (9 events) in his observations showed spinning motion at a few 10 km/s, consistent with prediction from numerical simulation. The direction of spin is also consistent with that of unwinding motion of helically twisted flux tubes observed in the same active region 7260. (Schmieder et al. 1995 and Kurokawa et al. 1987 observed similar spinning motion of surges. See also related numerical simulation by Karpen et

al. 1997 on the reconnection between sheared and un-sheared fields and resulting formation of cool jets. On the other hand, Priest et al. 1994 proposed the converging flux model as a model of X-ray bright points.)

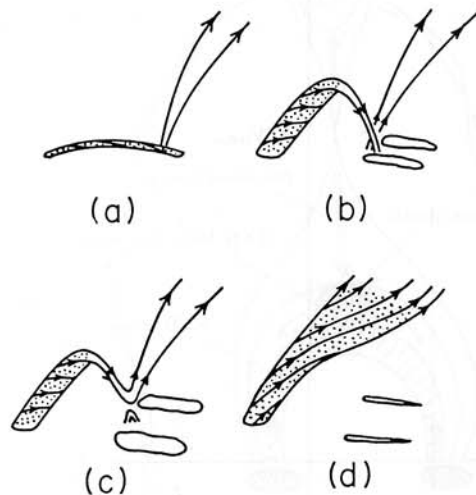


Figure 8. Schematic illustration of formation of a spinning magnetic-twist jet as a result of reconnection between a twisted flux tube and an untwisted flux tube (Shibata and Uchida 1986).

3. FLARES AND PLASMOIDS

3.1. LDE FLARES VS IMPULSIVE FLARES

Solar observers have long thought that there are two types of flares, e.g., long duration event (LDE) flares and impulsive flares. LDE flares typically last more than 1 hour, while impulsive flares are short lived, less than 1 hour. The latter is characterized by the impulsive hard X-ray emission whereas the former shows more softer X-ray spectrum.

Yohkoh soft X-ray telescope (SXT) has discovered that many LDE flares show *cusp-shaped loop* structures (Tsuneta et al. 1992, Hanaoka 1995, Tsuneta 1996, Forbes and Acton 1996; Fig. 9), which are quite similar to magnetic field configuration predicted by the classical magnetic reconnection model (Carmichael-Sturrock-Hirayama-Kopp-Pneuman model, called CSHKP model). There are a number of evidence of magnetic reconnection in these LDE flares (Tsuneta 1996): (1) The temperature is systematically higher in outer loops (see numerical simulations of reconnection coupled with heat conduction by Yokoyama and Shibata [1997a,b]). (2) The cusp-shaped loops apparently grow with time, i.e., the height of loops and the separation of two footpoints of loops increase with time. (3) The energy release rate and other physical quantities are consistent with the prediction by magnetic reconnection model. (4) The plasmoid ejections are often seen in the rise phase of LDE flares (e.g., Hudson 1994).

From these observations and analyses, it was established that LDE flares are produced by the CSHKP-type magnetic reconnection mechanism.

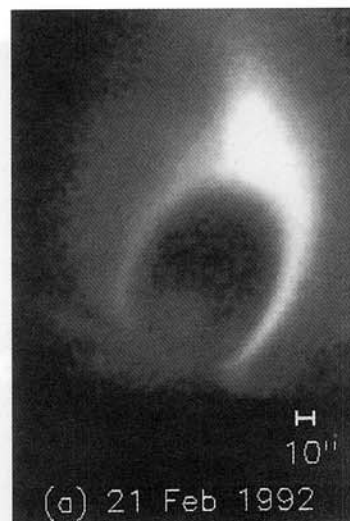


Figure 9. LDE flare on 21 Feb. 1992 observed with SXT (Tsuneta et al. 1992).

The SXT images of impulsive flares, however, show only *simple loop* structures, as already known from Skylab observations. Hence it was first thought that these impulsive flares might be created by the mechanism different from that for LDE flares, and the magnetic reconnection model was questioned.

It was Masuda (1994) who changed this situation dramatically. He carefully coaligned the SXT and the HXT (hard X-ray telescope; Kosugi et al. 1991) images of some impulsive compact loop flares observed at the limb, and showed that there is an impulsive HXR source *above* the SXR loop, in addition to the footpoint impulsive double HXR sources (Masuda et al. 1994, 1995; Fig. 10). Since the impulsive HXR sources are produced by high energy electrons which are closely related to the main energy release mechanism, this means that *the main energy release occurred above (outside) the SXR loop*. This means also that the flare models invoking the energy release site inside the SXR loops (e.g., Alfvén and Carlqvist 1967, Spicer 1977, Uchida and Shibata 1988) must now be discarded at least for these impulsive compact loop flares.

What is the energy release mechanism in these compact loop flares? Masuda et al. (1995) postulated that the basic magnetic field configuration is similar to that of LDE flares and that the high speed jet produced by the reconnection collides with the top of the reconnected loop to produce very hot region as well as high energy electrons. (See Aschwanden et al. 1996 for independent observational evidence for acceleration site of high energy electrons high above the SXR loops.)

3.2. X-RAY PLASMOID EJECTIONS FROM IMPULSIVE FLARES

If the impulsive compact loop flares occur as a result of reconnection in a geometry similar to that for LDE flares, plasmoid ejections would be observed high above the loop top HXR source (Fig. 11; see also Hirayama 1991, Moore and Roumeliotis 1992). Shibata et al. (1995) searched for such plasmoid ejection

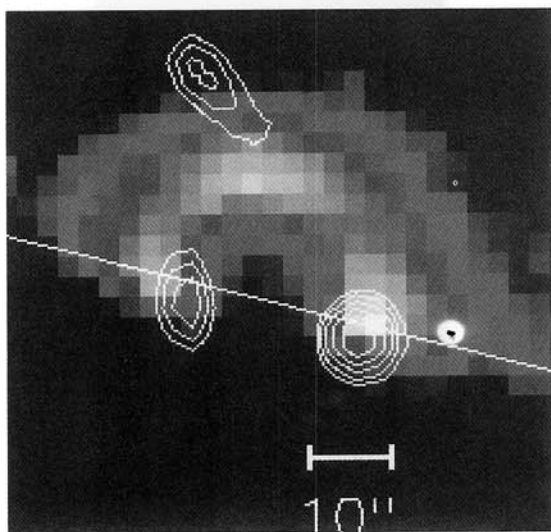


Figure 10. Impulsive flare on 13 Jan. 1992 which shows a loop top hard X-ray source above soft X-ray loop (Masuda et al. 1994). Contours of hard X-ray (33 – 53 keV) intensity distribution are overlaid on the soft X-ray (~ 1 keV) image.

tions using SXT images in 8 impulsive compact loop flares observed at the limb, which are selected by Masuda (1994) in an unbiased manner. They indeed found that *all these flares were associated with X-ray plasma (or plasmoid) ejections*. The apparent velocity of these ejections are 50 – 400 km/s, and their height ranges are $4 - 10 \times 10^4$ km. Interestingly, flares with HXR source well above the loop top show systematically higher velocity. The SXR intensity of the ejections is very low, typically $10^{-4} - 10^{-2}$ of the bright SXR loop. The shape of these plasma ejections is loop-like (e.g., 4 Oct 92 flare), blob-like (e.g., 5 Oct 92 flare [Ohyama and Shibata 1997b], see Fig. 12; 2 Dec 91 flare [Tsuneta 1997]), or jet-like (e.g., 13 Jan 92 flare), which are somewhat similar to the shape of CMEs (e.g., Burkepile and Cyr 1993). In many cases, strong acceleration of plasmoids occur during the impulsive phase (Ohyama and Shibata 1997a,b, Fig. 13), and the temporal relation between height of the ejections and the HXR intensity is very similar to that between CME height and the SXR intensity of an associated flare.

Ohyama and Shibata (1997a,b) and Tsuneta (1997) analyzed the temperature distribution of plasmoids, flare loops, and ambient structure, and have revealed that the temperature of plasmoids is $\sim 6 - 13$ MK, less than that of flare loops, and the overall temperature distribution is consistent with that predicted by the reconnection model.

Ohyama and Shibata (1997a,b) showed that the kinetic energy of plasmoids is much smaller than that of the total flare energy. This means that the kinetic energy of the plasmoid ejection cannot be the source of flare energy. Instead, the plasmoid ejection could play a role to trigger the main energy release in impulsive phase, since in some events observed from the preflare phase it was found that the plasmoid ejection started (at 10 km/s) well before the impulsive phase

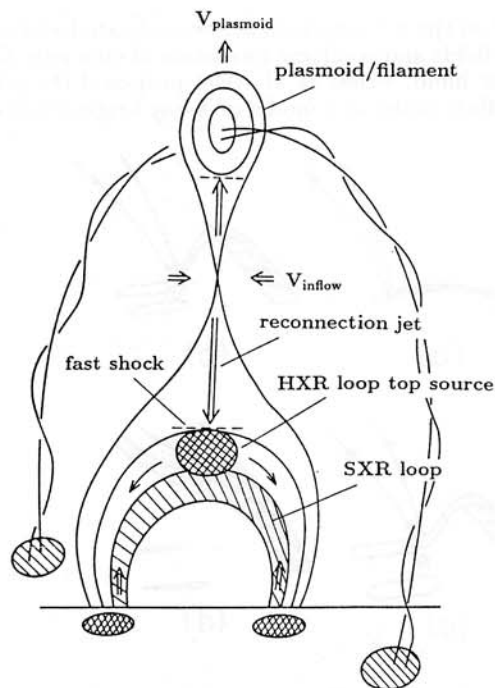


Figure 11. A unified model of flares: plasmoid-induced-reconnection model (Shibata et al. 1995, Shibata 1996a,b, 1997a,b).

(Ohyama and Shibata 1997a; Fig. 13).

3.3. RECONNECTION MODEL: PLASMROID-INDUCED-RECONNECTION MODEL

On the basis of above observations, Shibata (1996a,b, 1997a,b) proposed the *plasmoid-induced-reconnection model*, by extending the classical CSHKP model. In this model, the plasmoid ejection plays a key role to trigger fast reconnection (see Fig. 11).

Let us consider the situation that a plasmoid suddenly rises at velocity $V_{plasmoid}$.² Since the plasma density does not change much during the eruption process, the plasma inflow

$$V_{inflow} \sim V_{plasmoid} L_{plasmoid} / L_{inflow}$$

must develop toward the X-point to compensate the mass ejected by the plasmoid, where $L_{plasmoid}$ and $L_{inflow} (> L_{plasmoid})$ are the typical sizes of the plasmoid and the inflow. We consider that the impulsive phase correspond to the phase when $L_{inflow} \sim L_{plasmoid}$, i.e.,

$$V_{inflow} \sim V_{plasmoid} \sim 50 - 400 \text{ km/s.}$$

²In this model, on the basis of observations, we assume that the plasmoid is already created before the flare, and is suddenly accelerated by some mechanism. Magnetic reconnection might also play a role in such preflare phase as noted by Ohyama and Shibata (1997a). See also related theoretical studies by Kusano et al. (1995), Kitabata et al. (1996), Magara et al. (1997).

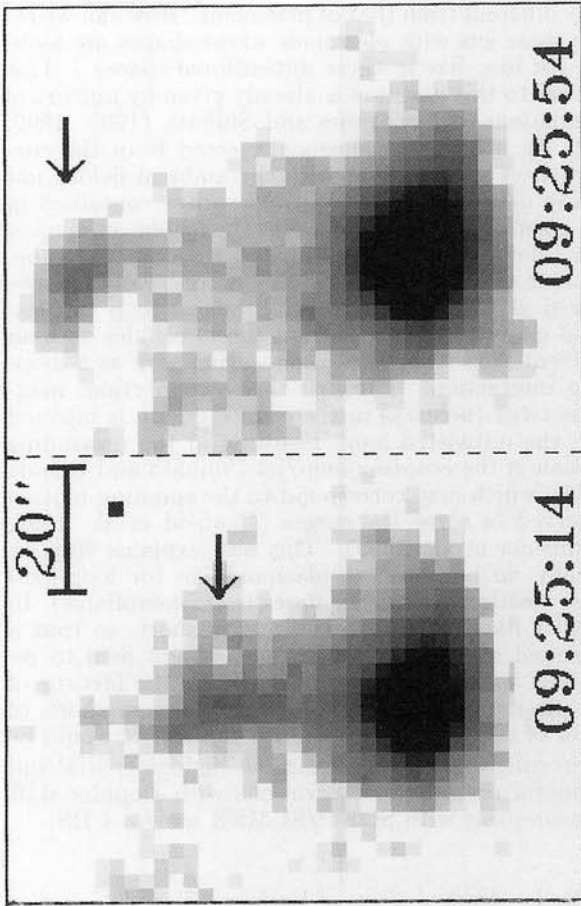


Figure 12. X-ray plasmoid ejections from an impulsive compact loop flare observed with Yohkoh SXT on 5 Oct. 1992 (Ohyama and Shibata 1996, 1997b). The velocity of the ejections is 200 – 450 km/s.

Since the reconnection rate is determined by the inflow speed, the ultimate origin of fast reconnection in this model is the fast ejection of the plasmoid. After the impulsive phase, we expect that L_{inflow} becomes larger than $L_{plasmoid}$ because the distance between the plasmoid and the X-point increases, and hence the inflow speed V_{inflow} would decrease much, leading to slow reconnection which corresponds to the decay or late phase.

In this model, the electric field at the X-point (and surrounding region) becomes $E \sim V_{inflow} B/c$ and is largest during impulsive phase. Hence, it naturally explains acceleration of higher energy electrons in impulsive phase than in decay phase.

The magnetic reconnection theory predicts two oppositely directed high speed jets from the reconnection point at Alfvén speed,

$$V_{jet} \sim V_A \simeq 2000 \left(\frac{B}{100G} \right) \left(\frac{n_e}{10^{10} \text{cm}^{-3}} \right)^{-1/2} \text{ km/s},$$

where B is the magnetic flux density and n_e is the electron density. The downward jet collides with the top of the SXR loop, producing MHD fast shock, superhot plasmas and/or high energy electrons at the

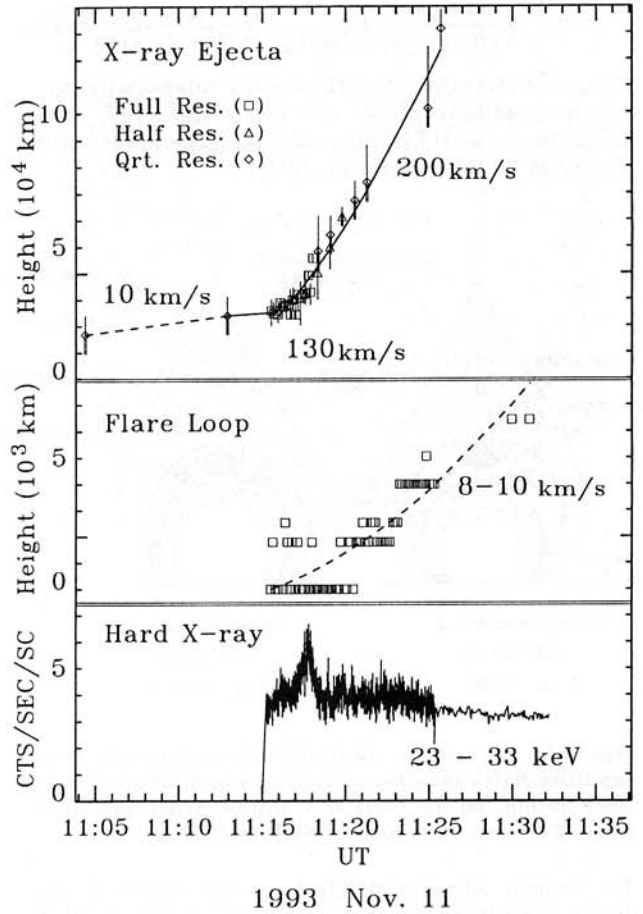


Figure 13. Temporal variations of the height of an X-ray plasmoid and the hard X-ray intensity in an impulsive flare on 11 Nov. 1993 observed by Yohkoh SXT and HXT (from Ohyama and Shibata 1997a).

loop top, as observed in the HXR images. The temperature just behind the fast shock becomes

$$T_{loop-top} \sim m_i V_{jet}^2 / (6k) \sim 2 \times 10^8 \left(\frac{B}{100G} \right)^2 \left(\frac{n_e}{10^{10} \text{cm}^{-3}} \right)^{-1} \text{ K},$$

where m_i is the hydrogen ion mass and k is the Boltzmann constant. This explains the observationally estimated temperature of the loop top HXR source (Masuda 1994). We would expect similar physical process for the upward directed jet (see Fig. 11). Indeed we find a SXR bright point during the impulsive phase somewhat far from the SXR loop. This bright point seems to be located at the footpoint of the erupting loop.

The magnetic energy stored around the current sheet and the plasmoid is suddenly released through reconnection into kinetic and thermal/nonthermal energies after the plasmoid is ejected. The magnetic energy release rate at the current sheet (with the length of $L_{inflow} \sim L_{plasmoid} \simeq 2 \times 10^4$ km) is estimated to be

$$dW/dt = 2 \times L_{plasmoid}^2 B^2 V_{inflow} / 4\pi$$

$$\sim 4 \times 10^{28} \left(\frac{V_{inflow}}{100 \text{ km/s}} \right) \left(\frac{B}{100 \text{ G}} \right)^2 \left(\frac{L_{plasmoid}}{2 \times 10^9 \text{ cm}} \right)^2 \text{ erg/s.}$$

This is comparable with the energy release rate during the impulsive phase, $4 - 100 \times 10^{27}$ erg/s, estimated from the HXR data, assuming the lower cutoff energy as 20 keV (Masuda 1994).

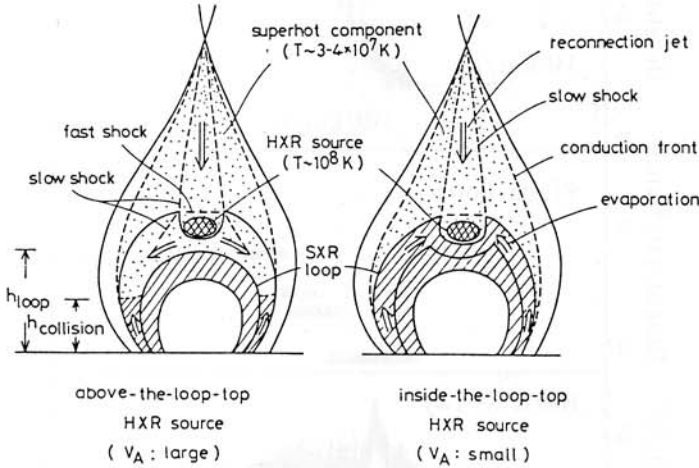


Figure 14. Schematic illustration to explain why some impulsive flares show above-the-loop-top HXR source and other do not, on the basis of a unified model (plasmoid-induced-reconnection model) (Shibata 1997b).

The reason why the HXR loop top source is not bright in SXR is that the evaporation flow (e.g., Hori et al. 1997, Yokoyama and Shibata 1997b) has not yet reached the colliding point and hence the electron density (and so the emission measure) is low. The key physical parameter discriminating impulsive flares and LDE flares (or impulsive phase and gradual phase) is the velocity of the inflow, V_{inflow} . If V_{inflow} is large, the reconnection is fast, so that the reconnected field lines accumulate very fast and hence the MHD fast shock (i.e., HXR loop top source) is created well above SXR loop which is filled with evaporated plasmas. On the other hand, if V_{inflow} is small, the reconnection is slow and hence the fast shock is produced at the SXR loop (see Fig. 14).

4. SUMMARY: UNIFIED VIEW AND UNIFIED MODEL

As we have seen above, Yohkoh SXT/HXT observations have revealed various evidence of magnetic reconnection, especially common occurrence of X-ray mass ejections (plasmoids and/or jets), in LDE flares, impulsive flares, and microflares. These are summarized in Table 1.

On the basis of this unified view, Shibata (1996a,b, 1997a,b) proposed a unified model, *plasmoid-induced-reconnection model*, to explain not only LDE and impulsive flares but also microflares and X-ray jets. That is, equations derived in the previous section can be applied to all these flares.

One may argue, however, that the shape of X-ray jets and $H\alpha$ surges (i.e., collimated jet-like structure) is

very different from that of plasmoids. How can we relate these jets with plasmoids whose shapes are blob-like (or loop-like in three dimensional space)? This answer to this question is already given by numerical simulations of Yokoyama and Shibata (1995, 1996; Fig. 6); a blob-like plasmoid ejected from the current sheet soon collides with the ambient fields, and finally disappears (Fig. 15). The mass contained in the plasmoid is transferred into the reconnected open flux tube and forms a collimated jet along the tube. In three dimensional space, this process would be observed as follows: an erupting helical loop (a plasmoid ejected from the current sheet) collides with an ambient loop to induce reconnection seen as a loop-loop interaction. Through this reconnection, magnetic twist (helicity) in the erupting loop is injected into the untwisted loop, resulting in the unwinding motion of the erupting loop/jet (Shibata and Uchida 1986), which may correspond to the spinning motion observed in some $H\alpha$ surges (Canfield et al. 1996, Schmieder et al. 1995). This also explains why we usually do not observe plasmoid-like (or loop-like) mass ejections in smaller flares (e.g., microflares). In smaller flares, the current sheet is short, so that a plasmoid soon collides with an ambient field to reconnect with it and disappear. Hence the lifetime of the plasmoid (or loop-like) ejection is very short, of order of $t \sim L/V_{plasmoid} \sim 10 - 100$ sec. It would be interesting to test this scenario using high spatial and temporal resolution observations with Doppler shift measurement with SOHO/SUMER and/or CDS.

Table I Unified View of Various "Flares"

"flares"	mass ejections (cool)	mass ejections (hot)
giant arcades	$H\alpha$ filament eruptions	CMEs
LDE flares	$H\alpha$ filament eruptions	X-ray plasmoid ejections/CMEs
impulsive flares	$H\alpha$ sprays	X-ray plasmoid ejections
transient brightenings (microflares)	$H\alpha$ surges	X-ray jets
EUV microflares	surges/spicules	EUV jets
facular points (nanoflares ?)	spicules	(Alfven waves)

Finally, we note that the essentially the same physical process (magnetic reconnection associated with plasmoid ejections) can occur even below the transition region (see Table 1 and Fig. 16). If the reconnection occur in the upper chromosphere, the temperature of heated plasma is of order of $10^5 - 10^6$ since the

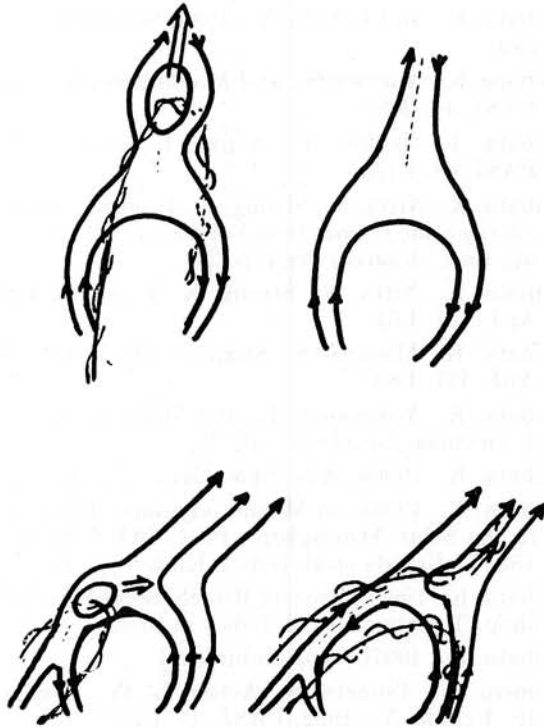


Figure 15. Unification of CSHKP model and emerging flux model by the plasmoid-induced-reconnection model (Shibata 1997a,b). Note that a plasmoid (a magnetic island or a helically twisted flux rope) collides and reconnects with the ambient magnetic field to disappear in a short time scale (10 - 100 sec) in the case of small scale flares such as microflares.

pre-heated plasma temperature is low ($\sim 10^4$ K) and the local plasma $\beta (= p_{gas}/p_{mag})$ is not low (> 0.01); note that the temperature of the reconnection-heated plasma is $\sim T_0/\beta$. EUV explosive events/jets (e.g., Dere et al. 1991, Innes et al. 1997) may correspond to these reconnection events. If the reconnection occurs in the photosphere as suggested by recent MDI results (Title and Tarbel 1997 in these proceedings), we would observe photospheric bright points (nanoflares) as well as mass flow with a velocity of a few - 10 km/s. This impulsive mass flow as well as large amplitude Alfvén waves generated by the reconnection could be a source of energy to produce spicules and coronal heating (Kudoh and Shibata 1997).

ACKNOWLEDGMENTS

The author would like to thank T. Kudoh, M. Ohyama, M. Shimojo, T. Yokoyama and other Yokoh colleagues for their various help and interesting discussion.

REFERENCES

Acshwanden, M. J., Hudson, H. S., Kosugi, T., and Schwartz, R. A., 1996, *ApJ*, 464, 985.
Acton, L., et al., 1992, *Science*, 258, 618.

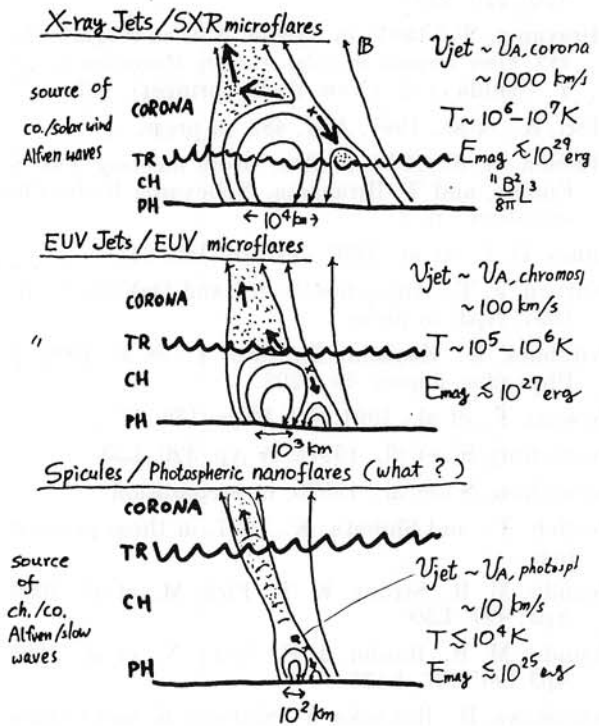


Figure 16. Various jet phenomena in quiet regions of the Sun; X-ray jets/SXR microflares, EUV jets/EUV microflares, and spicules/photospheric nanoflares. All these jet phenomena may be generated by magnetic reconnection. Note also that the reconnection is a source of large amplitude (high frequency) Alfvén waves.

Alfvén, H., and Carlqvist, P. 1967, *Sol. Phys.* 1, 220.
Aurass, H., Klein, K. -L., and Martens, P. C. H., 1995, *Solar Phys. Lett.*, 155, 203.
Biskamp, D., 1997, *Phys. Plasma*, 4, 1964.
Burkepile, J.T., Cyr, O.C.St., 1993, A Revised and Expanded Catalogue of Mass Ejections Observed by the Solar Maximum Mission Coronagraph. HAO.
Brueckner, G. E., and Bartoe, J. -D. F., 1983, *ApJ*, 272, 329.
Canfield, R. C., Reardon, K. P., Leka, K. D., Shibata, K., Yokoyama, T., and Shimojo, M., 1996, *ApJ*, 464, 1016.
Cook, J. W. and Brueckner, G. E., 1991, in *Solar Interior and Atmosphere*, A. N. Cox et al. (eds.), Univ. Arizona Press, p. 996.
Dennis, B. R., 1985, *Solar Phys.*, 100, 465.
Dere, K., et al., 1991, *JGR*, 96, 9399.
Forbes, T., Acton, L. 1996, *ApJ*, 459, 330.
Forbes, T. G. and Priest, E. R. 1984, *Solar Phys.*, 94, 315.
Gopalswamy, N., Payne, T. E. W., Schmahl, E. J., et al., 1994, *ApJ*, 437, 522.
Hanaoka, Y., 1994, in *Proc. Kofu meeting*, eds. S. Enome, and T. Hirayama, Nobeyama Radio Observatory, p. 181.
Hanaoka, Y., 1996, *Solar Phys.*, 165, 275.

- Heyvaerts, J., Priest, E. R. and Rust, D. M., 1977, *ApJ*, 216, 123.
- Hirayama, T., 1991, in *Lecture Note in Physics, No. 387, Flare Physics in Solar Activity Maximum 22*, ed. Y. Uchida et al. (New York, Springer), 197.
- Hori, K., et al., 1997, *ApJ*, 489, in press.
- Hudson, H. S., 1994, in Proc. Kofu meeting, eds. S. Enome, and T. Hirayama, Nobeyama Radio Observatory, p. 1.
- Innes, D. E., et al., 1997, *Nature*, 386, 811.
- Karpen, J. T., Antiochos, S. K., and DeVore, C. R., 1997, *ApJ*, in press.
- Kitabata, H., Hayashi, T., Sato, T., et al. 1996, *J. Phys. Soc. Japan*, 65, 3208.
- Kosugi, T., et al., 1991, *Sol. Phys.* 136, 17.
- Koutchmy, S., et al., 1997a, *A Ap*, 320, L33.
- Koutchmy, S., et al., 1997b, in preparation.
- Kudoh, T., and Shibata, K., 1997, in these proceedings.
- Kundu, M. R., Strong, K. T., Pick, M., et al., 1994, *ApJ*, 427, L59.
- Kundu, M. R., Raulin, J. P., Nitta, N., et al., 1995, *ApJ Let*, 447, L135.
- Kurokawa, H., Hanaoka, Y., Shibata, K. and Uchida, Y., 1987, *Solar Phys.*, 108, 251.
- Kusano, K., Suzuki, Y., and Nishikawa, K. 1995, *ApJ*, 441, 942.
- Lin, R. P., et al., 1984, *ApJ*, 283, 421.
- Magara, T., Shibata, K., Yokoyama, T., 1997, *ApJ*, in press.
- Masuda, S., 1994, Ph. D. Thesis, U. Tokyo.
- Masuda, S., Kosugi, T., Hara, H., Tsuneta, S., and Ogawara, Y., 1994, *Nature*, 371, 495.
- Masuda, S., Kosugi, T., Hara, H., et al., 1995, *PASJ*, 47, 677.
- Moore, R. L., and Roumeliotis, G. 1992, in *Lecture Note in Physics, No. 399, Eruptive Flares*, ed. Z. Svestka, B. V. Jackson, and M. E. Machado (New York, Springer), 69.
- Nitta, N., 1996, Proc. Bath Conf., Observations of Magnetic Reconnection in the Solar Atmosphere, Bentley, R. and Mariska, J. T. (eds.), ASP conf. ser., vol. 111, p. 156.
- Ohyama, M., and Shibata, K. 1997a, *PASJ*, 49, 249.
- Ohyama, M., and Shibata, K. 1997b, *ApJ*, submitted.
- Okubo, A. et al., 1996, Proc. Bath Conf., Observations of Magnetic Reconnection in the Solar Atmosphere, Bentley, R. and Mariska, J. T. (eds.), ASP conf. ser., vol. 111, p. 39.
- Ono, Y., et al., 1996, *Phys. Rev. Lett.* 76, 3328.
- Porter, J. G., Fontenla, J. M., Simnett, G. M., 1995, *ApJ*, 438, 472.
- Priest, E. R., Parnell, C. E., and Martin, S. F., 1994, *ApJ*, 427, 459.
- Raulin, J. P., Kundu, M. R., Hudson, H. S. et al., 1996, *AA*, 306, 299.
- Schmieder, B., K. Shibata, L. van Driel-Gesztelyi, and S. Freeland, 1995, *Solar Phys.*, 156, 245.
- Scholer, M., 1989, *JGR*, 94, 8805.
- Shibata, K., and Uchida, Y., 1986, *Solar Phys.*, 103, 299.
- Shibata, K., Nozawa, S., and Matsumoto, R., 1992a, *PASJ*, 44, 265.
- Shibata, K., Ishido, Y., Acton, L., et al., 1992b, *PASJ*, 44, L173.
- Shibata, K., Nitta, N., Strong, K. T., et al., 1994a, in *"X-ray Solar Physics from Yohkoh"*, eds. Y. Uchida et al., *Univ. Academy Press*, p. 29.
- Shibata, K., Nitta, N., Strong, K. T., et al., 1994b, *ApJ*, 431, L51.
- Shibata, K., Masuda, S., Shimojo, M., et al., 1995, *ApJ*, 451, L83.
- Shibata, K., Yokoyama, T., and Shimojo, M., 1996, *J. Geomag. Geoelectr.*, 48, 19.
- Shibata, K., 1996a, *Adv. Space Res.*, 17, (4/5)9.
- Shibata, K., 1996b, in *Magnetodynamic Phenomena in the Solar Atmosphere*, Proc. IAU Colloq. No. 153, Y. Uchida et al. (eds.), Kluwer, p. 13.
- Shibata, K., 1997a, Proc. of Hitachi Solar Flare workshop, T. Sakurai et al. (eds.) in press.
- Shibata, K., 1997b, *ApJ*, submitted.
- Shimizu, T., Tsuneta, S., Acton, L. W., Lemen, J. R., Uchida, Y., 1992, *PASJ*, 44, L147.
- Shimizu, T., et al., 1994, *ApJ*, 422, 906.
- Shimizu, T., 1995, *PASJ*, 47, 251.
- Shimizu, T., 1996, Ph. D. Thesis, U. Tokyo.
- Shimojo, M., Hashimoto, S., Shibata, K., et al., 1996, *PASJ*, 48, 123.
- Shimojo, M., Harvey, K. K., Shibata, K., 1997, *Solar Phys.*, in press.
- Spicer, D. 1977, *Sol. Phys.*, 53, 305.
- Sterling, A.C., Shibata, K., and Mariska, J.T., 1993, *ApJ*, 407, 778
- Strong, K. T., Harvey, K., Hirayama, T., et al., 1992, *PASJ*, 44, L161.
- Suematsu, Y., Wang, H., & Zirin, H., 1995, *ApJ*, 450, 411
- Tajima, T., and Shibata, K., 1997, *Plasma Astrophysics*, Addison-Wesley, in press.
- Tsuneta, S., et al., 1991, *Solar Phys.*, 136, 37.
- Tsuneta, S., et al., 1992, *PASJ*, 44, L211.
- Tsuneta, S., 1996, *ApJ*, 456, 840.
- Tsuneta, S., et al. 1997, *ApJ*, 478, 787.
- Tsuneta, S., 1997, *ApJ*, 483, 507.
- Uchida, Y. and Shibata, K., 1988, *Sol. Phys.*, 116, 291.
- Ugai, M., 1986, *Phys. Fluids*, 29, 3659.
- Ugai, M., 1994, *Phys. Plasma*, 1, 2853.
- Watanabe, T., 1994, in Proc. Kofu meeting, eds. S. Enome, and T. Hirayama, Nobeyama Radio Observatory, p. 99.
- Yokoyama, T., and Shibata, K., 1994, *ApJ*, 436, L197.
- Yokoyama, T., and Shibata, K., 1995, *Nature*, 375, 42.
- Yokoyama, T., and Shibata, K., 1996, *PASJ*, 48, 353.
- Yokoyama, T., and Shibata, K., 1997a, *ApJ*, 474, L61.
- Yokoyama, T., and Shibata, K., 1997b, in these proceedings.